Patient-Specific Atrial Simulations Reproducing Clinical Electrogram Biomarkers Under Pacing Stress Protocol

Duna de Luis-Moura[1], Chiara Celotto[2], Saman Golmaryami[3], María Termenón-Rivas[1], Giada S Romitti[1], Santiago Moreno-Pineda[1], Etel Silva[3], Juan Fernandez-Armenta[3], José F Rodriguez[2], Alejandro Liberos[1], Miguel Rodrigo[1]

[1]CoMMLab, Universitat de València,València, Spain
[2]Department of Chemistry Giulio Natta, Politecnico di Milano, Milano
[3]Department of Cardiology, Hospital Universitario Puerta del Mar, Cádiz, Spain

Abstract

Digital twins offer a framework to study atrial substrate, but their ability to reproduce intracardiac electrogram biomarkers used to guide therapy is not fully established. We analyzed five patients with persistent atrial fibrillation, projecting 1,363 clinical bipolar electrograms onto a patient-specific digital twin of the left atrium. The model was calibrated using a triple extrastimulus pacing protocol, including adjustments of conduction properties and structural remodeling. This calibrated framework was then used to generate 21,527 simulated bipolar electrograms with integrated fibrosis. Electrograms were analyzed in a 290 ms window following a triple extrastimulus pacing protocol, extracting activation duration, number of deflections, and local activation time variability. Aberrant regions consistently showed increased activation duration in both datasets (simulations: 91 to 130 ms; clinical: 134 to 193 ms), together with consistent increases in deflections (sim: 5.6 to 7.4; clinical: 11.4 to 20.9) and LAT variability (sim: 3.5 to 5.8 ms; clinical: 11.4 to 21.9 ms). These findings demonstrate that patient-specific atrial models can reproduce electrophysiological patterns and may support identification of conduction abnormalities.

1. Introduction

Atrial fibrillation (AF) is the most common sustained cardiac arrhythmia and is thought to be partly sustained by aberrant electrical propagation within a remodeled atrial substrate, including regions of fibrosis and slow conduction. While pulmonary vein isolation is effective for paroxysmal AF, persistent forms are often maintained by complex structural and electrophysiological abnormalities [1].

Patient-specific computational models provide a powerful framework to investigate the atrial substrate in detail [2], enabling the simulation of electrical activation and the generation of virtual electrograms (EGMs). Although bipolar electrograms are widely used in clinical practice to characterize atrial conduction, they are rarely reproduced or validated in patient-specific computational models. Direct comparison between simulated and annotated clinical bipolar electrograms is therefore essential to assess the ability of patient-specific models to reproduce observed atrial activation patterns.

In our previous work, we developed a pipeline to generate patient-specific atrial models electrophysiologically calibrated to clinical local activation time maps [3]. However, that framework did not incorporate fibrosis modeling nor enable the generation of simulated electrograms for direct comparison with clinical data. In the present study, we extend this approach by integrating fibrosis into the models and generating simulated bipolar electrograms. We then compare simulated and clinical signals and evaluate whether features extracted from the simulations, such as the number of deflections and activation duration, can help identify regions of potentially abnormal atrial substrate.

2. Methods

2.1. Patient-specific atrial models

Five patient-specific three-dimensional models of the left atrium were generated from pre-procedural CT images segmented using ADAS 3D software. Endocardial and epicardial surfaces were reconstructed and used to generate volumetric tetrahedral meshes. Fiber orientation and anatomical heterogeneity were incorporated using an atlas-based methodology [4].

Fibrotic regions were estimated from clinical bipolar peak-to-peak voltage maps derived from intracardiac electrograms. Nodes in low-voltage areas were identified as structurally abnormal, while intermediate voltage values were used to assign a probability of fibrosis at each node. Spatially coherent fibrotic patterns aligned

with myocardial fiber orientation were then generated using a probabilistic algorithm [5]. Structural and electrophysiological remodeling was subsequently applied within these areas, incorporating partial uncoupling and altered conduction properties to reflect the functional impact of fibrosis on atrial propagation [6].

To unmask conduction abnormalities, a triple extra-stimulus pacing protocol (3-Extra) was applied both clinically and in the simulations. This protocol consists of three premature stimuli delivered during sinus rhythm with progressively decreasing coupling intervals [1]. As in clinical practice, the atrial response to the third extrastimulus (S3) was used for subsequent analysis.

Electrophysiological properties were then incorporated into the models using a previously described calibration procedure [3], adapted here to reproduce the activation patterns observed after S3 within a patient-specific substrate already including fiber orientation, tissue differentiation and fibrotic remodeling. First, a global diffusion coefficient was adjusted to match the overall propagation pattern of the clinical local activation time (LAT) map. Subsequently, spatially heterogeneous conduction properties were introduced through local diffusion adjustments based on the regional LAT error between simulated and clinical maps. Electrical remodeling was then incorporated, and the configuration minimizing the LAT error for S3 was selected (Figure 1).

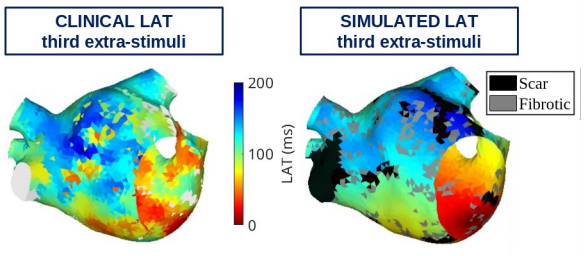

Figure 1. Clinical (left) and simulated (right) local activation time (LAT) maps of the atrial response to the S3 stimulus.

Electrophysiological simulations were performed using a GPU-accelerated monodomain solver with the Koivumäki atrial cellular model to obtain activation patterns and transmembrane potentials for each model [8; 9]. Simulations also reproduced the location and duration of the stimulation applied during the clinical procedure.

2.2. Electrogram analysis

To enable electrogram computation, a reduced endocardial surface (~3000 nodes) was extracted from the volumetric mesh and used as virtual electrode locations. Unipolar electrograms were computed from the simulated transmembrane potentials using a standard forward model. From these signals, bipolar electrograms were calculated.

In clinical practice, electrograms are classified as aberrant or non-aberrant based on the morphology of the atrial response to S3 in the 3-Extra protocol. Aberrant electrograms were visually inspected and defined as fragmented signals with four or more peaks and duration over 40 ms or highly fragmented with more than 5 peaks and over 63 ms [1]. These clinically defined labels were used as reference to evaluate the ability of the simulations to reproduce patterns associated with abnormal conduction.

Clinical electrode locations were first projected onto the reduced simulated endocardial electrode mesh previously aligned to the patient-specific atrial model. Simulated bipolar electrograms were then constructed by generating all possible pairs of simulated electrodes satisfying an inter-electrode distance of 0.8–2.5 mm. For each valid pair, the midpoint was computed and used as a spatial reference.

Clinical labels were assigned to each simulated electrode pair by identifying the nearest projected clinical node within a 5 mm radius of the midpoint. If no clinical node was found within this distance, the simulated pair was discarded. This procedure ensured a one-to-one correspondence between simulated bipolar electrograms and clinically annotated regions (Figure 2). Simulated bipolar electrograms were obtained by subtracting the corresponding unipolar signals.

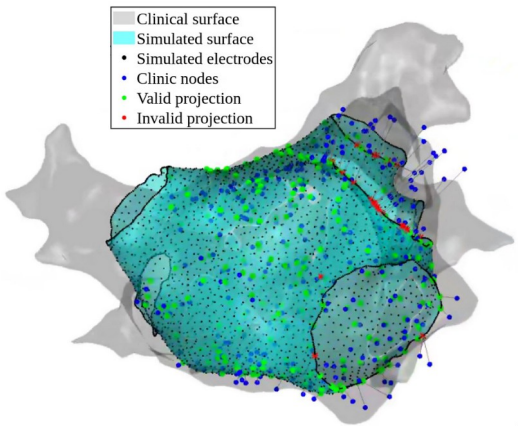

Figure 2. Projection of clinical nodes from the clinical mesh (gray) onto the reduced simulated electrode mesh (cyan), where simulated electrodes are shown as black dots. Each clinical node (blue) is associated with its nearest simulated electrode, illustrated by a connecting black line. Nodes satisfying the distance criterion are considered valid projections (green), whereas nodes exceeding the threshold are labeled as invalid (red asterisk).

Both clinical and simulated signals were band-pass filtered (0.5–300 Hz) to reduce noise. A 290 ms analysis window was then extracted, starting 10 ms after S3, to

capture the atrial response to the pacing protocol. Representative examples of healthy and aberrant electrograms are shown in Figure 3.

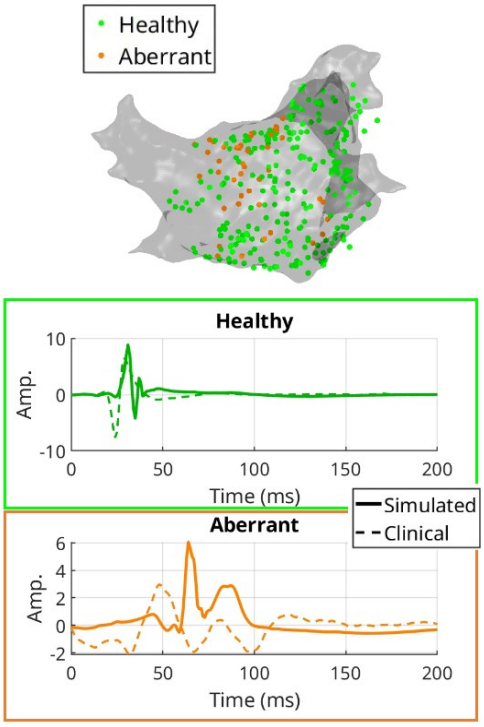

Figure 3. Examples of clinical and simulated EGMs. The upper panel shows the clinical mesh with labels assigned to each electrode. The lower panel presents representative simulated (solid line) and clinical (dashed line) electrograms for healthy (green) and aberrant (orange) regions.

From all those signals, three features were extracted within this window for both clinical and simulated signals: activation duration, number of deflections and LAT variability.

Activation duration was computed using relative amplitude thresholds (1% for simulated signals; 5% onset and 2% offset for clinical signals), and measured as the time interval in which the absolute value of the bipolar EGM exceded these thresholds.

The number of deflections was estimated from the first derivative of the signal by identifying zero-crossings corresponding to local extrema. A relative amplitude threshold was applied to the derivative (10% for simulated and 25% for clinical signals) to suppress noise-induced detections.

LAT variability was quantified as the standard deviation of LAT at bipolar EGMs within a radius of 8 mm. On average, simulated nodes had 39.75 ± 15.99 neighbors, whereas clinical nodes had 4.03 ± 2.65 neighbors due to the difference in node density between both meshes.

3. Results

3.1. Simulated vs clinical electrograms dataset

For N=5 patients, a total of 1,363 clinical bipolar electrograms were analyzed including 1,238 healthy and 125 aberrant signals. Using the proposed spatial matching criteria, 21,527 simulated bipolar electrograms were generated, of which 18,969 were labeled as healthy and 2,558 as aberrant.

The spatial correspondence between clinical and simulated electrograms was quantified by measuring the distance between the midpoint of each simulated electrode pair and its associated clinical node (Figure 2). The average matching distance was 1.93 ± 0.46 mm. Each simulated electrode pair was used only once to ensure independent comparisons across locations.

3.1. Electrogram features in healthy vs aberrant regions

Simulated electrograms reproduced consistent differences between healthy and aberrant regions across all evaluated features. In both clinical and simulated data, aberrant regions exhibited longer activation duration, a higher number of deflections, and increased LAT spatial variability. Activation duration increased from 91.31 ± 78.85 ms to 130.32 ± 69.10 ms in simulations and from 133.91 ± 111.01 ms to 193.31 ± 92.59 ms in clinical recordings. Similarly, the number of deflections increased from 5.58 ± 3.06 to 7.42 ± 3.81 in simulations and from 11.36 ± 9.58 to 20.94 ± 14.46 in clinical signals. LAT spatial variability also increased from 3.47 ± 1.16 ms to 5.77 ± 3.37 ms in simulations and from 11.40 ± 8.19 ms to 21.87 ± 13.09 ms in clinical data. Boxplots for each metric are shown in Figure 4.

However, the magnitude of these differences was consistently lower in simulations. Absolute values were reduced, and the separation between healthy and aberrant regions was less pronounced compared to clinical data.

4. Discussion

These results demonstrate that patient-specific atrial digital twins calibrated using clinical activation data can reproduce key qualitative features of intracardiac bipolar electrograms. The calibration strategy combines global and local adjustments of conduction properties and ionic remodelling based on LAT discrepancies, together with fibrosis integration derived from clinical voltage maps, enabling patient-specific propagation under a clinical pacing protocol.

Simulated electrograms were directly compared with

clinically annotated bipolar electrograms used for atrial substrate characterization. In both datasets, abnormal regions consistently exhibited prolonged activation, increased fragmentation, and higher LAT variability. However, these effects were attenuated in simulations, with reduced absolute values and lower separation between normal and abnormal regions.

This discrepancy likely arises from modeling simplifications, with locally-uniform conditions such as fiber direction or tissue type, and the absence of other atrial structures such as ganglionated plexi or fat infiltration. These factors reduce signal complexity and may underestimate fine-scale conduction heterogeneity and electrogram fractionation.

Despite these limitations, the framework provides a direct mapping between simulated and clinical electrograms through a shared spatial labeling approach, enabling the evaluation of clinically relevant electrogram biomarkers. From a clinical perspective, this supports the use of patient-specific digital twins as a tool to explore atrial conduction patterns under controlled pacing conditions and potentially assist in identifying regions associated with abnormal conduction.

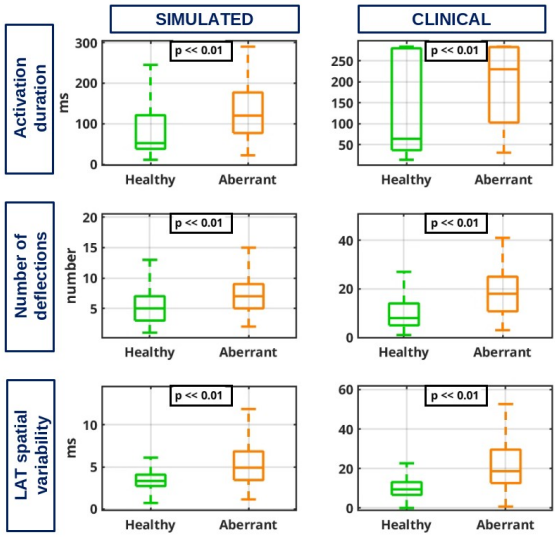

Figure 4. Boxplots of the evaluated features for clinical and simulated electrograms, comparing non-aberrant (green) and aberrant (orange) regions.

5. Conclusions

Patient-specific atrial digital twins calibrated using clinical activation data can reproduce key electrophysiological differences between normal and abnormal regions observed in intracardiac bipolar electrograms, including activation prolongation, increased fragmentation, and higher LAT variability.

The proposed framework enables the integration of clinically derived electrogram biomarkers into simulation-based models, providing a step toward patient-specific tools that may support the identification of conduction abnormalities and guide targeted atrial fibrillation treatment strategies.

Acknowledgments

This work was funded by Generalitat Valenciana Grant AICO/2021/318 (Consolidables 2021), Grants PID2020-114291RB-I00, PID2023-148702OB-I00 and EraNet PCI2024-153442 funded by MCIN/ 10.13039/501100011033 and by "ERDF A way of making Europe".

References

[1] E. Silva Garcia, I. Lobo-Torres, J. Fernandez-Armenta, D. Penela, M. Fernandez-Garcia, A. Gomez-Lopez, …, and A. Berruezo, "Functional mapping to reveal slow conduction and substrate progression in atrial fibrillation," Europace, vol. 25, no. 11, Art. no. euad246, 2023.

[2] N. A. Trayanova and K. C. Chang, "How computer simulations of the human heart can improve anti-arrhythmia therapy," J. Physiol., vol. 594, no. 9, pp. 2483–2502, 2016.

[3] D. De Luis-Moura, C. Celotto, S. S. Golmaryami, M. Termenón-Rivas, G. S. Romitti, E. Silva Garcia, J. Fernandez-Armenta, J. Rodriguez Matas, A. Liberos, and M. Rodrigo, "Personalised models of atrial propagation fitted to clinically-induced activation maps," in Proc. Comput. in Cardiol. (CinC), vol. 52, 2025, pp. 1–4.

[4] G. S. Romitti, A. Liberos, M. Termenón-Rivas, J. Barrios-Álvarez de Arcaya, and M. Rodrigo, "Asignación de dirección de fibra y tipo celular en anatomías auriculares personalizadas mediante coordenadas baricéntricas," in XLII Congreso Anual de la Sociedad Española de Ingeniería Biomédica, 2024.

[5] M. Termenón-Rivas, G. S. Romitti, D. De Luis-Moura, D. Calvo, N. Pérez Castellano, A. Liberos, and M. Rodrigo, "Estimación de la distribución fibrótica auricular a partir de medidas de voltaje en electrogramas," in XLIII Congreso Anual de la Sociedad Española de Ingeniería Biomédica, 2025.

[6] G. S. Romitti, M. Termenón-Rivas, A. Liberos, and M. Rodrigo, "Modelling Fibrosis Infiltration in a Virtual Cohort: Impact on Atrial Fibrillation Vulnerability" in Proc. Comput. in Cardiol. (CinC), vol. 52, 2025, pp. 1–4

[7] V. M. García-Molla, A. Liberos, A. Vidal, M. S. Guillem, J. Millet, A. Gonzalez, …, and A. M. Climent, "Adaptive step ODE algorithms for the 3D simulation of electric heart activity with graphics processing units," Comput. Biol. Med., vol. 44, pp. 15–26, 2014.

[8] J. T. Koivumäki, G. Seemann, M. M. Maleckar, and P. Tavi, "In silico screening of the key cellular remodeling targets in chronic atrial fibrillation," PLoS Comput. Biol., vol. 10, no. 5, Art. no. e1003620, 2014.

Address for correspondence:
Miguel Rodrigo (miguel.rodrigo@uv.es)
Av. de la Universitat s/n 46100 Burjassot. Valencia. Spain.